Highly Stretchable and UV Curable Elastomers for Digital Light Processing Based 3D Printing

Dinesh K. Patel, Amir Hosein Sakhaei, Michael Layani, Biao Zhang, Qi Ge, and Shlomo Magdassi**

Additive manufacturing (AM) which is commonly referred to 3D printing, has gained great attention in recent years as it allows the creation of complex 3D geometries with precisely prescribed microarchitectures, which enable new functionalities or improved performance. Compared to other existing 3D printing technologies, such as fused deposition modeling (FDM), Polyjet, selective laser sintering (SLS), direct ink writing (DIW), and stereolithography (SLA), the digital light processing (DLP) technique is considered as a low cost, high throughput additive manufacturing technique. DLP printing is based on localized photopolymerization process which is triggered by UV radiation and takes place within a bath containing liquid monomers, oligomers, and photoinitiators. It is capable of generating a variety of highly complex, 3D structures from micro- to mesoscales with microscale architecture and submicrometer precision.[1] In addition, as the printing process takes place in a liquid environment, the DLP printing technique does not require any support materials to print porous and hollow structures, which makes this an ideal solution to fabricating lattice metamaterials,[2,3] pneumatically actuated soft robots,[4,5] and many other structures and devices constructed with trusses or cavities.[6,7] Over the last few years, researchers have made exciting advances in DLP 3D printing technology, such as projection micro-stereolithography providing micro/sub-micrometer printing resolution,[1,8] continuous liquid interface production enabling 100 times faster printing,[9] and large-area projection micro-stereolithography creating 3D features spanning seven orders of magnitude from nanometers to centimeters.[3] However, so far the studies on developing DLP compatible high-performance, multifunctional materials are comparatively very limited.[10,11]

Elastomers, due to their excellent material properties of elasticity, resilience, and electrical and thermal insulation, have been used in myriad of applications including automotive bumpers, rubber seals, flexible electronics, energy absorbers, and many others. In addition, elastomers are also considered as ideal materials for fabricating soft robots[12–14] and smart biomedical devices[15,16] which require soft and deformable material properties to establish safe and smooth interactions with humans, externally and internally. The most widely used elastomers in these applications are silicon rubber, that is, Ecoflex (Smooth-On), SE 1700 (Dow Corning), and Sylgard (Dow Corning). However, the thermal curing process of these silicon rubbers constrains the fabrication of objects to only traditional ways, such as cutting, molding/casting, spin-coating, etc. In order to enrich the design and fabrication flexibility, researchers have developed a few direct ink writing (DIW) based methods to 3D print silicon rubbers[17–19] by developing printing inks which are composed of two parts of a silicone elastomer, that is, base and cross-linker with an expensive platinum-based catalyst.[20–22] However, after printing out the two parts, a few hours curing process is still needed at room temperature.[19] In addition, the lateral resolution of the DIW technique is determined by the size of the printing nozzle which is at hundreds micrometer scale, and the requirement of support materials in the case of printing overhanging structures significantly constrains the structure complexity. In addition to the thermal curable silicon rubbers, there are a few commercially available UV curable elastomers that are suitable for UV curing related 3D printing techniques such as digital light processing (DLP), stereolithography (SLA), and Polyjet. These UV curable elastomers include Carbon EPU 40,[23] Stratasys TangoPlus,[24] Formlab Flexible,[25] and Spot-A Elastic.[26] However, compared to silicon rubbers, those UV curable elastomers still have very significant limitations. First, the highest elongation at break of these elastomers is about 170–220%,[24] which is not sufficient for certain advanced applications. Second, as they are commercial product, users are not able to tune the mechanical properties, that is, the Young's modulus. In addition, in order to guarantee the printing resolution, light absorbing dyes are usually added to these commercial resins, which results in opaque printed objects and therefore are not applicable in applications requiring good light transmittance.

Here, we report a family of highly stretchable and UV curable (SUV) elastomer systems that are suitable for UV radiation based 3D printing. We present here printing with a DLP

Dr. D. K. Patel, Prof. S. Magdassi
Casali Center for Applied Chemistry
Institute of Chemistry
The Center for Nanoscience and Nanotechnology
The Hebrew University of Jerusalem
Jerusalem 9190401, Israel
E-mail: magdassi@mail.huji.ac.il

Dr. A. H. Sakhaei, Dr. B. Zhang, Prof. Q. Ge
Digital Manufacturing and Design Center
Singapore University of Technology and Design
Singapore 487372, Singapore
E-mail: ge_qi@sutd.edu.sg

Dr. M. Layani
School of Materials Science and Engineering
Nanyang Technological University
Singapore 639798, Singapore

Prof. Q. Ge
Science and Math Cluster
Singapore University of Technology and Design
Singapore 487372, Singapore

DOI: 10.1002/adma.201606000

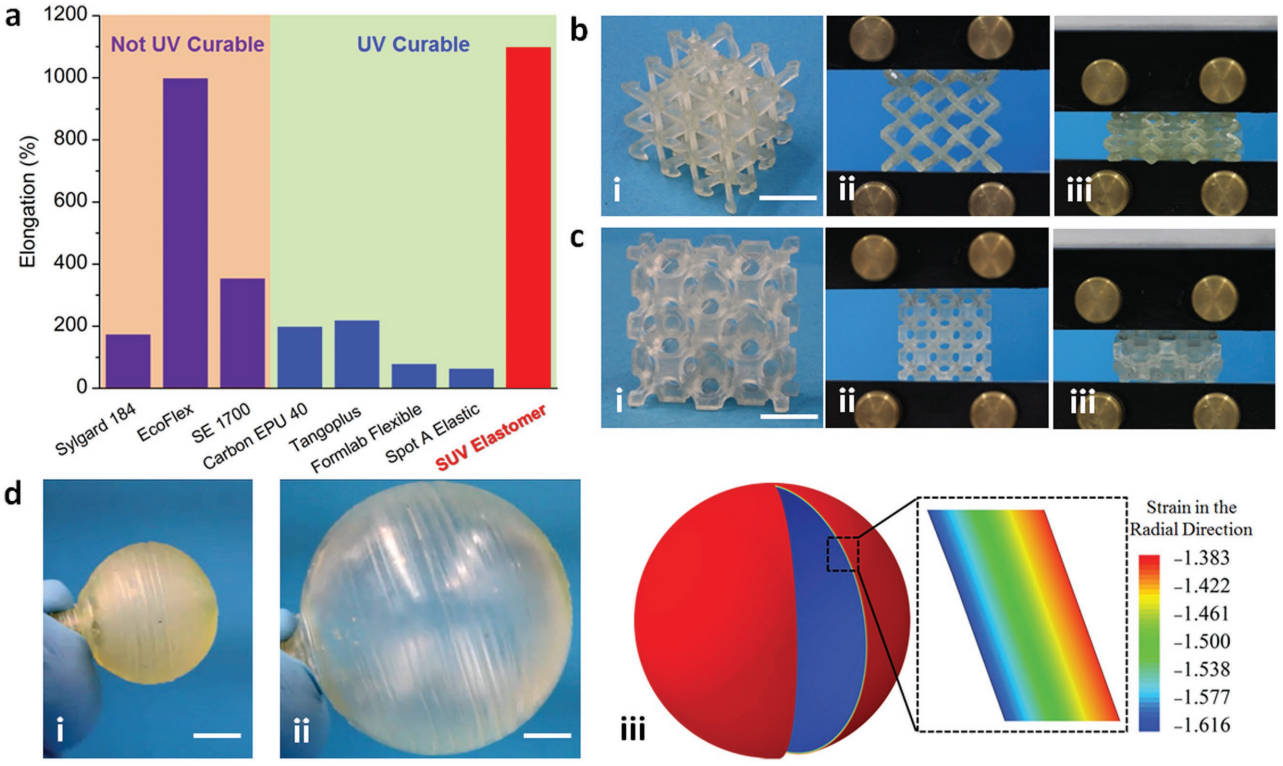

Figure 1. Highly stretchable and UV (SUV) curable elastomers. a) Comparison of elongation at break between not UV curable silicone rubbers, commercially available UV curable elastomers, and our SUV elastomer. b) A 3D printed highly deformable isotropic truss: (i) isometric perspective view, and (ii) the undeformed shape and (iii) deformed shape in a compressive test. c) A 3D printed highly deformable negative Poisson's ratio structure: (i) front view, and (ii) the undeformed shape and (iii) deformed shape in a compressive test. d) A 3D printed highly deformable balloon: (i) undeformed shape, (ii) inflated into three times the original size, and (iii) an FEA simulation indicates that in the radial direction, the balloon's wall was compressed by ≈160%. The scale bar is 10 mm.

printer, but the same compositions are suitable for a variety of UV 3D printers, such as SLA, Polyjet, and dispensing, while adjusting the viscosity. The DLP printable SUV elastomer resin formulations were prepared by mixing a monofunctional monomer consisting of epoxy aliphatic acrylate (EAA), and a difunctional cross-linker consisting of aliphatic urethane diacrylate (AUD) diluted with 33 wt% of isobornyl acrylate (Figure S1, Supporting Information). The AUD oligomer is comprised of "soft domains" made up of aliphatic chains, and "hard domains" made up of urethane units. Hydrogen bonds mainly form between N—H groups and C=O groups on the hard domains.[27–29] The detailed chemical structures are presented in Table S1, Figures S1–S3 (Supporting Information). By mixing EAA and AUD with different ratios, we are able to readily tune the mechanical properties for different applications. The elastomer composition contains 2% of trimethyl benzoyl diphenyl phosphine oxide (TPO) as photoinitiator, that is suitable for use in low-cost DLP printers[30] and also in two-photon polymerization printers.[31,32] The printed elastomers can be stretched by up to 1100% (**Figure 1**a shows comparison with available elastomers) which is more than five times the elongation at break of the commercial UV curable elastomers and is competitive to that of the most stretchable silicon rubber. Using DLP-based 3D printing technique with our SUV elastomers, we are able to directly create complex 3D lattice structures such as an isotropic truss structure[33] (Figure 1b), negative Poisson's ratio structure[34] (Figure 1c), and hollow structures such as a printed balloon (Figure 1d) exhibiting extremely large deformation (Movie S1, Supporting Information), which previously could be fabricated only by combining traditional methods with 3D printing.[34,35] The SUV elastomer system reported in this paper will significantly enhance the capability of the DLP-based 3D printing for fabricating soft and deformable 3D structures and devices including soft robots and actuators, flexible electronics, acoustic metamaterials, and in many other applications.

Figure 2a presents the hyperelastic behavior of the SUV system with EAA-AUD mixing ratio ranging from 5:5 to 0:10. It was observed that the increase in the AUD cross-linker concentration not only leads to the increase in Young's modulus from 0.58 to 4.21 MPa, but also significantly increases the elongation at break from ≈240 to ≈1100% which is about five times that of the best existing commercial UV curable elastomers.[24] We note that in the SUV system, the elongation at break increases with increasing in the cross-linker concentration, and this trend is opposite to that of a normal thermoset system.[10,36,37] We attribute the high stretchability to the presence of hydrogen bonds (Figure S4, Supporting Information) between hard domains of the AUD.[27–29] Upon mechanical loading, the breakage of hydrogen bonds dissipates energy and therefore results in the high stretchability of the elastomer system.[38] Adding more EAA into the elastomer system does not only reduce the cross-linking density, but also narrows

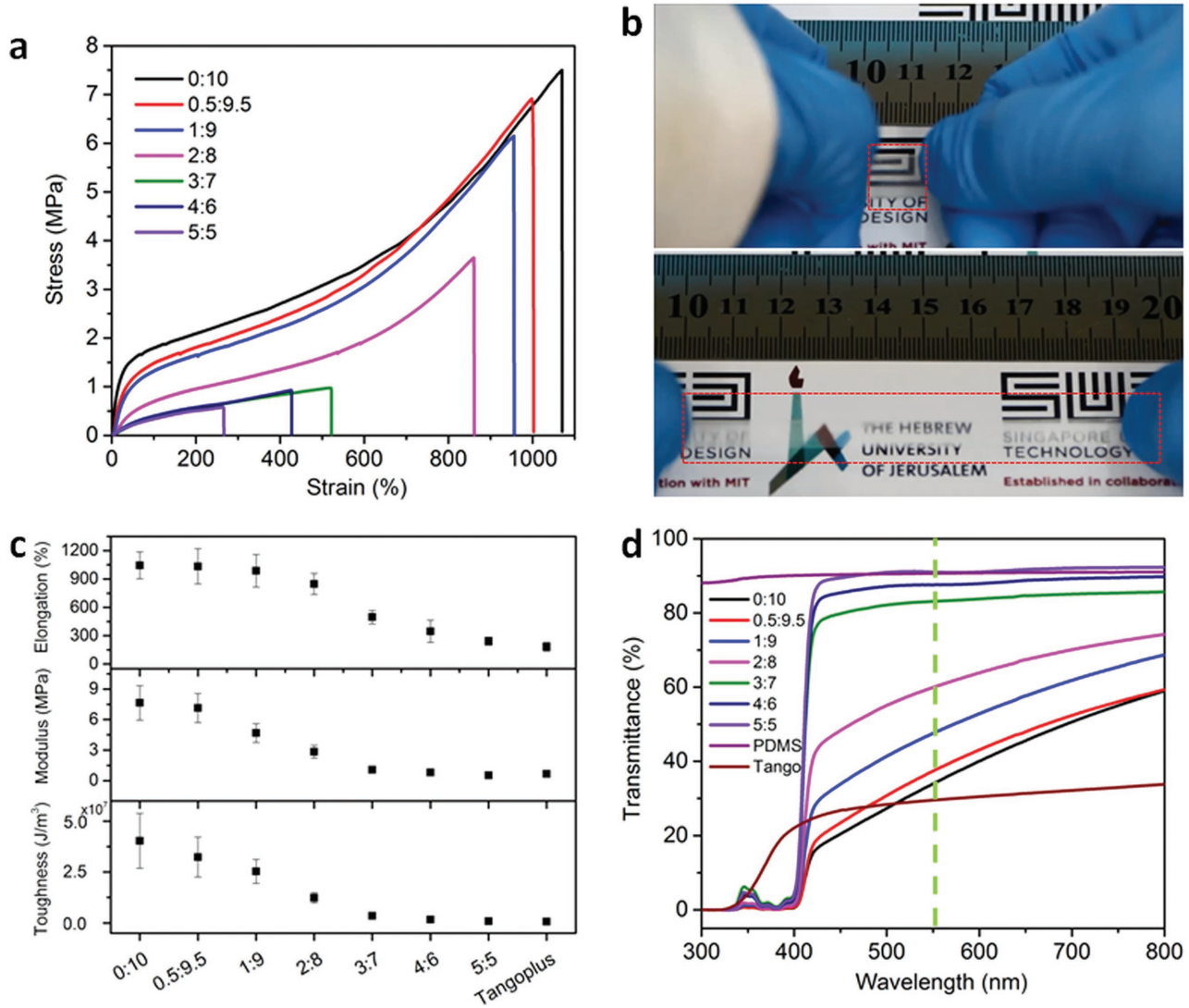

Figure 2. Material properties of SUV elastomer system. a) Highly stretchable stress–strain behavior of the SUV elastomers with various EAA-AUD ratios. b) Snapshots of stretching a transparent SUV elastomer specimen by about ten times. c) Comparisons on stretchability, Young's modulus, and toughness between SUV elastomers and TangoPlus. d) Comparisons on light transmittance between SUV elastomers and other commercially available elastomers.

the distribution of the hard segments of the cross-linked network,[39] which significantly reduces the presence of the hydrogen bonds, therefore decreases the system's stretchability as well as stiffness. We proved this assertion by carrying out uniaxial loading–unloading cyclic tests using elastomers prepared with different EAA-AUD mixing ratios (Figure S5, Supporting Information). Figure 2b shows snapshots of examining the high stretchability of a transparent elastomer sample with the 0:10 mixing ratio (Movie S2, Supporting Information). In Figure 2c, we compare the elongation at break, Young's modulus, and the material toughness extracted from the stress–strain curves of the elastomers with different compositions. By integrating the stress–strain curves in Figure 2a, we found that the toughness varies from 1×10^6 to 50×10^6 J m^{-3} with the mixing ratio from 5:5 to 0:10. In comparison, the mechanical properties of the typical and highly used commercial printable elastomer, TangoPlus, broke at ≈190% with Young's modulus 0.6 MPa and toughness 0.9×10^6 J m^{-3}. Along with good mechanical properties, the new SUV elastomer system also possesses a good optical property. Figure 2d shows the material's light transmittance at 300–800 nm. The SUV elastomers are opaque to UV light (below 400 nm), which is attributed to the UV light absorption by the TPO photoinitiator[30] and partly by the oligomer (Figure S6, Supporting Information). Within the light range of 400–800 nm, the transmittance of the SUV elastomers increases with the increase in the EAA monomer concentration. By comparing the transmittance at 550 nm, it can be seen that the transmittance increases from 34 to 91.6% with the EAA-AUD mixing ratio from 0:10 to 5:5, which is comparable to that of the commonly used transparent elastomer polydimethylsiloxane (PDMS) (90.6%) that has found a myriad of applications in optical devices.[40,41] The transparency is also higher than that of the commercial TangoPlus elastomer (≈30%).

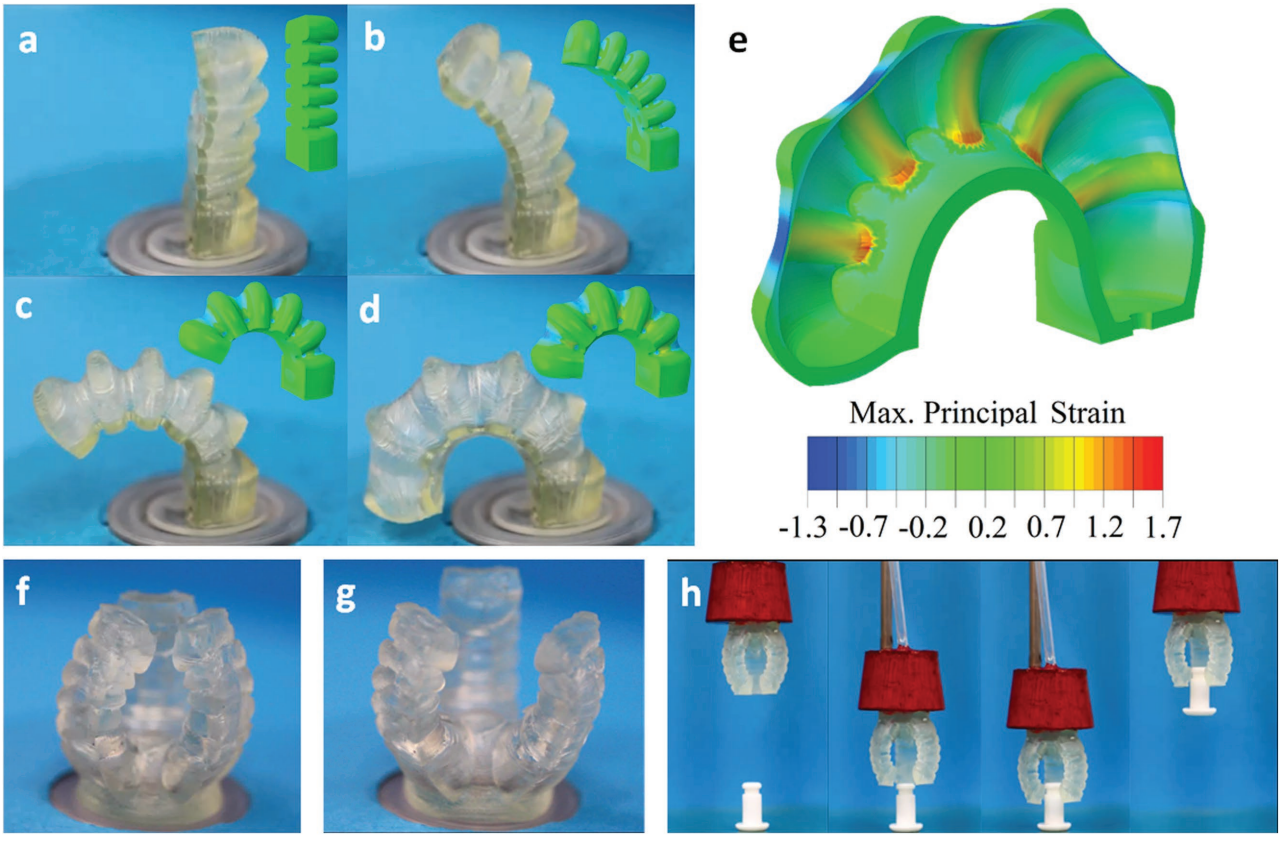

Figure 3. 3D printed pneumatically actuated soft actuators. a–d) Snapshot of a soft actuator exhibits large deformation bending under pressurized air along with FEA simulations. e) FEA simulation reveals large local deformation. f) A 3D printed gripper opens in g) under pressurized air. h) The 3D printed gripper is in process of grabbing an object.

Overall, the new highly stretchable elastomer system is very suitable for the DLP-based 3D printing technique that has advantages including high printing resolution, fast processing speed, and high freedom of design of very delicate structures as will be shown below. In addition, this technique does not require support materials for printing porous/hollow structures, which is crucial for 3D printing delicate structures, as the process of removing the support materials might cause severe damage to the printed structures. Using our DLP printable SUV elastomers, we are able to print highly deformable and complex 3D structures which have not been achieved by any other approaches. In the following, we will present 3D printed soft actuators and Bucky ball electronic switches to demonstrate the unique strengths of the SUV elastomer system.

Recently, the emerging field of soft robots has gained considerable attention as they are composed of soft, elastic, flexible components that provide multiple degrees of freedom and many useful capabilities including the ability to exhibit large deformation, establish safe and smooth interaction with humans, manipulate delicate objects, and conform to irregular surrounding geometries. Currently, researchers are mainly using silicon rubber such as Ecoflex and Sylgard-184, to fabricate soft robots.[12,14,42–45] However, currently the complex, multistep molding and casting manufacturing approach, significantly constrains the geometric complexity and functionality of the created soft robots. To overcome these challenges, there are a few attempts[4,5] to use 3D printing methods to fabricate soft robots, while the mechanical performance of the printable soft material, especially stretchability, becomes a major challenge to enhance the functionality of soft robots.[5] The SUV elastomer developed in this paper provides a key solution to developing complex 3D functional soft robots within a simple, single, and rapid 3D printing step. **Figure 3** demonstrates pneumatically actuated soft actuators fabricated using DLP 3D printing. Compared to previous studies, the excellent stretchability of this elastomer results in 3D printed soft actuators that exhibit much larger bending deformation (Figure 3a–d, Movie S3, Supporting Information). In Figure 3e, the finite element (FE) simulation reveals that the local strain increases to ≈170% when the straight actuator deforms into a half circle. This could not be realized by printing a similar soft actuator with a comparatively brittle commercial elastomer which breaks at 50%.[5] In Figure 3f–h, we demonstrate a completely 3D printed soft gripper (Figure 3f) which is actuated by pressurized air (Figure 3g, Movie S4, Supporting Information) and in the process of grasping an object (Figure 3h, Movie S5, Supporting Information). It should be noted that using the one-step 3D printing method to fabricate such a 3D soft gripper significantly reduces the fabrication complexity and time. By the traditional molding and casting method, it is impossible to build a complete 3D mold that can be used to replicate the entire 3D gripper. Therefore, until now, additional time-consuming

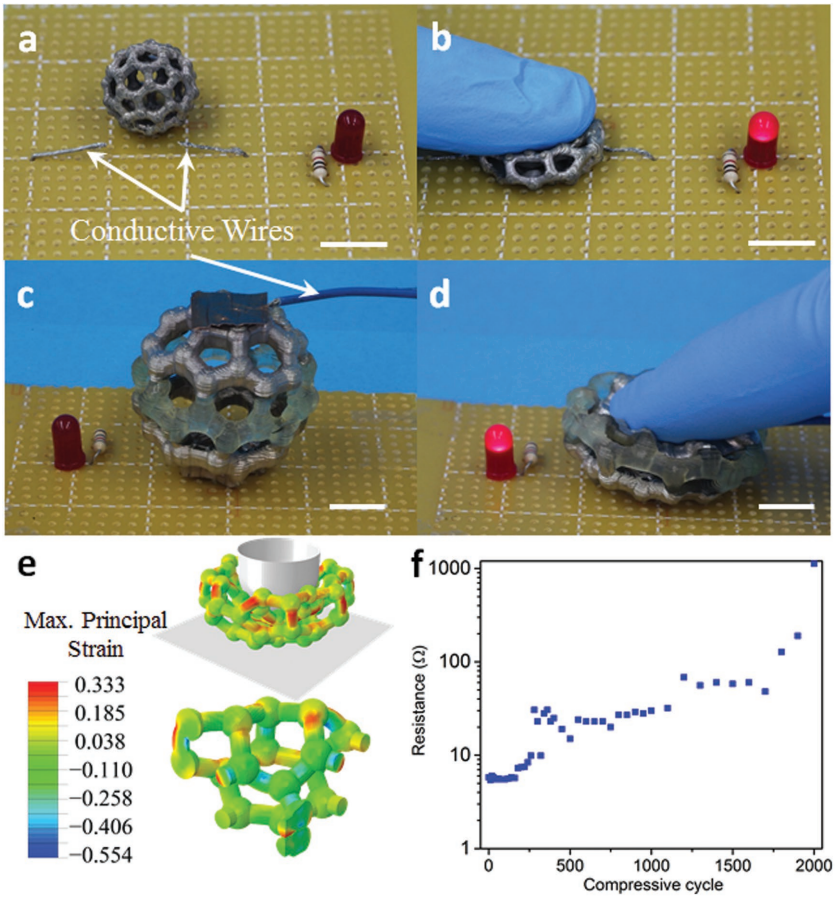

Figure 4. Conductive Bucky balls working as an electric switch. a) A Bucky ball completely coated with silver nanoparticles. b) A LED turns on after compressing the Bucky ball. c) A Bucky ball selectively coated with silver nanoparticles. d) A LED turns on after compressing the selectively coated Bucky ball. e) Finite element simulation. f) Bucky ball's conductivity under 2000 times cyclic compressive testing. The scale bar is 10 mm.

assembly steps must be employed to assemble all the separate molded parts.

Not only do our SUV elastomers sustain large elastic deformation, but also maintain a good mechanical repeatability over more than 1000 times of loading/unloading cycles. Based on this, we fabricated a 3D Bucky ball light switch by combining the DLP printing with a silver nanoparticle coating and a room-temperature sintering process.[11,46–48] As shown in **Figure 4**a, a deformable Bucky ball with the C_{60} chemical structure[49] was printed. To achieve the electrical conductivity, we coated the Bucky ball with silver nanoparticles by immersing it into a silver nanoparticles dispersion, and exposed the coated Bucky ball to hydrogen chloride vapors.[50] Figure 4a shows a Bucky ball that is fully covered by the sintered silver nanoparticles. We demonstrate the Bucky ball as a switch by mounting it onto a circuit board where the conductive wires are not connected. After compressing the ball, the deformed Bucky ball bridged the two disconnected wires to form a complete circuit, and the light-emitting diode (LED) turned on (Figure 4b). After releasing the compressive force, the Bucky ball returned to the original shape due to good elasticity, and the LED turned off as the circuit disconnected (Movie S6, Supporting Information). In Figure 4c, we also selectively coated Bucky ball where a nonconductive layer is sandwiched between two conductive layers which are connected to two separated conductive wires. After compressing the ball, the two conductive layers contacted each other, which completes the circuit and turns on the LED light (Figure 4d, Movie S7, Supporting Information). An FEA simulation was conducted to simulate this compressing/uncompressing process. In Figure 4e, the strain contour shows that the maximum local deformation occurs at the middle of the Bucky ball where it is bent most. The maximum compressive strain is only about 55% even when the two conductive layers are in contact, which ensures the compressed ball stays within the safe elastic region without damaging it. To examine the Bucky ball's electric repeatability, we conducted a cyclic compressive test by repeatedly compressing the ball over 2000 times (Movie S8, Supporting Information). An ohmmeter was connected to the silver coating of the Bucky ball to measure the resistance change during the cyclic test. As shown in Figure 4f, within 1700 compressive loading/unloading cycles, the resistance increases from 6 Ω to around 60 Ω, and it increases to 190 Ω after 1900 cycles. A dramatic increase to 1100 Ω in resistance is observed only after 2000 cycles implying most likely a slight mechanical failure on the silver coating or the Bucky ball. Overall, the excellent mechanical and electric repeatability make the silver nanoparticle coated Bucky ball a good candidate in the field of 3D printed electronics, but further improvement of this layer is required. Obviously, coating the structure with other conductive materials such carbon nanotubes and metal nanowires will overcome the mechanical failure of the conductive layer, and it may be even used as a pressure sensor.

In summary, we report a family of highly stretchable and UV curable elastomers that are suitable for the DLP-based direct 3D printing technology. By mixing EAA and AUD at various ratios, we developed DLP printable elastomers that can be stretched by up to 1100% which is more than five times the elongation at break of the commercial UV curable elastomers. Using DLP printing with the SUV elastomer compositions enables the direct creation of complex 3D lattices or hollow structures that exhibit extremely large deformation. The SUV elastomer system will significantly enhance the capability of the DLP-based 3D printing of fabricating soft and deformable 3D structures and devices including soft actuators and robots, flexible electronics, acoustic metamaterials, and many other applications.

Experimental Section

Material Preparation: The SUV elastomer polymer resin was prepared by mixing AUD (Ebecryl 8413, Allnex) and EAA (Ebecryl 113, Allnex)

with a certain mixing ratio from 0:10 to 5:5. 2% TPO (BASF) of total weight of the polymer resin was added as the photoinitiator. The PDMS samples were made by mixing Elastrosil RT 601 A & B (Wacker) in 9:1 ratio at 70 °C for 30 min. TangoPlus samples were printed by Objet 260 Connex printer 3D printer, Stratasys using TangoPlus (FLX930, translucent).

Characterization: The mechanical properties were measured using Universal Testing Machine (INSTRON 3345, 500 N load cell). The dimensions of the specimens are about 50 mm × 5 mm × 0.75. The transmittance was measured using UV spectrophotometer (UV-1800, Shimadzu). The cyclic compressive tests were performed using homemade compression instrument, and resistance was measured during and after compressive cycles using Aim TTi BS 407 ohmmeter ranging from 1 μΩ to 20 kΩ. The photos and videos were recorded using Canon camera EOS 1200D equipped with Tamron SP Di macrolens.

3D Printing: 3D printing was performed using DLP-based 3D printer (Free form Plus 39, Asiga) with a custom-made heat resin bath and bath was maintained at 70 °C during printing process.[11] This printer operates by a top-down DLP system with a digital mirror device (DMD) and a UV–LED light source (385 nm). Each layer was irradiated for 10 s and layer thickness was 100 μm. The printed structures were sonicated with isopropyl alcohol (IPA) for 3 min to remove uncured monomer/oligomer followed by a 3 min postcuring in a UV oven. Isotropic truss, negative Poisson's ratio structure, soft actuator, gripper, and Bucky balls were printed using the SUV elastomer with composition 5:5.

Silver Coating on Printed Structure: The 3D printed structures, that is, the Bucky balls, were immersed in a silver dispersion in the dipropylene glycol methyl ether (DPM) solvent containing 16.5 wt% silver nanoparticles (Xjet Ltd., Israel). The process was performed in a vacuum chamber for 1 min. The immersed structures were then removed from the dispersion and dried in a vacuum oven at 50 °C for 30 min to evaporate the solvent. In order to achieve conductivity, the structures with silver nanoparticles were exposed to hydrogen chloride vapor for 10 s.[50]

Simulation: To investigate the local strains on the deformed 3D structures, the finite element simulations were performed using a commercial FE software ABAQUS (Simulia, Providence, RI, USA). The geometries were meshed using four-node linear tetrahedron and hybrid elements (C3D4H) for all the elastomeric components of the printed structures. The Mooney–Rivlin model was used to capture the hyperelastic behavior of the SUV elastomers (Figure S7, Supporting Information).

Supporting Information

Supporting Information is available from the Wiley Online Library or from the author.

Acknowledgements

This research was partially supported by the National Research Foundation, Prime Minister's Office, Singapore under the CREATE program: Nanomaterials for Energy and Water Management, and by the Israel National Nanotechnology Initiative FTA project on functional coatings and printing. A.H.S., B.Z., and Q.G. acknowledge support from SUTD Digital Manufacturing and Design Centre (DManD), supported by the Singapore National Research Foundation. Q.G. acknowledges STUD Start-up Research Grant. We thank Sorpol Ltd., Israel and Allnex, Germany for providing Ebecryl 8413 and Ebecryl 113 samples.

Received: November 7, 2016
Revised: December 30, 2016
Published online:

[1] X. Zheng, J. Deotte, M. P. Alonso, G. R. Farquar, T. H. Weisgraber, S. Gemberling, H. Lee, N. Fang, C. M. Spadaccini, *Rev. Sci. Instrum.* **2012**, *83*, 125001.
[2] X. Y. Zheng, H. Lee, T. H. Weisgraber, M. Shusteff, J. DeOtte, E. B. Duoss, J. D. Kuntz, M. M. Biener, Q. Ge, J. A. Jackson, S. O. Kucheyev, N. X. Fang, C. M. Spadaccini, *Science* **2014**, *344*, 1373.
[3] X. Zheng, W. Smith, J. Jackson, B. Moran, H. Cui, D. Chen, J. Ye, N. Fang, N. Rodriguez, T. Weisgraber, C. M. Spadaccini, *Nat. Mater.* **2016**, *15*, 1100.
[4] R. MacCurdy, R. Katzschmann, Y. Kim, D. Rus, presented at *2016 IEEE Int. Conf. on Robotics and Automation (ICRA)*, Stockholm, Sweden, May **2016**.
[5] N. P. Bryan, J. W. Thomas, Z. Huichan, F. S. Robert, *Bioinspiration Biomimetics* **2015**, *10*, 055003.
[6] N. W. Bartlett, M. T. Tolley, J. T. B. Overvelde, J. C. Weaver, B. Mosadegh, K. Bertoldi, G. M. Whitesides, R. J. Wood, *Science* **2015**, *349*, 161.
[7] C. Pouya, J. T. B. Overvelde, M. Kolle, J. Aizenberg, K. Bertoldi, J. C. Weaver, P. Vukusic, *Adv. Opt. Mater.* **2016**, *4*, 99.
[8] C. Sun, N. Fang, D. M. Wu, X. Zhang, *Sens. Actuators, A* **2005**, *121*, 113.
[9] J. R. Tumbleston, D. Shirvanyants, N. Ermoshkin, R. Janusziewicz, A. R. Johnson, D. Kelly, K. Chen, R. Pinschmidt, J. P. Rolland, A. Ermoshkin, E. T. Samulski, J. M. DeSimone, *Science* **2015**, *347*, 1349.
[10] Q. Ge, A. H. Sakhaei, H. Lee, C. K. Dunn, N. X. Fang, M. L. Dunn, *Sci. Rep.* **2016**, *6*, 31110.
[11] M. Zarek, M. Layani, I. Cooperstein, E. Sachyani, D. Cohn, S. Magdassi, *Adv. Mater.* **2016**, *28*, 4449.
[12] B. Mosadegh, P. Polygerinos, C. Keplinger, S. Wennstedt, R. F. Shepherd, U. Gupta, J. Shim, K. Bertoldi, C. J. Walsh, G. M. Whitesides, *Adv. Funct. Mater.* **2014**, *24*, 2163.
[13] D. Yang, B. Mosadegh, A. Ainla, B. Lee, F. Khashai, Z. G. Suo, K. Bertoldi, G. M. Whitesides, *Adv. Mater.* **2015**, *27*, 6323.
[14] S. A. Morin, R. F. Shepherd, S. W. Kwok, A. A. Stokes, A. Nemiroski, G. M. Whitesides, *Science* **2012**, *337*, 828.
[15] E. T. Roche, A. Fabozzo, Y. Lee, P. Polygerinos, I. Friehs, L. Schuster, W. Whyte, A. M. C. Berazaluce, A. Bueno, N. Lang, M. J. N. Pereira, E. Feins, S. Wasserman, E. D. O'Cearbhaill, N. V. Vasilyev, D. J. Mooney, J. M. Karp, P. J. del Nido, C. J. Walsh, *Sci. Transl. Med.* **2015**, *7*, 306ra49.
[16] A. T. Asbeck, S. M. M. De Rossi, I. Galiana, Y. Ding, C. J. Walsh, *IEEE Rob. Autom. Mag.* **2014**, *21*, 22.
[17] T. J. Hinton, A. Hudson, K. Pusch, A. Lee, A. W. Feinberg, *ACS Biomater. Sci. Eng.* **2016**, *2*, 1781.
[18] D. B. Kolesky, K. A. Homan, M. A. Skylar-Scott, J. A. Lewis, *Proc. Natl. Acad. Sci. USA* **2016**, *113*, 3179.
[19] J. T. Muth, D. M. Vogt, R. L. Truby, Y. Menguc, D. B. Kolesky, R. J. Wood, J. A. Lewis, *Adv. Mater.* **2014**, *26*, 6307.
[20] A. A. S. Bhagat, P. Jothimuthu, I. Papautsky, *Lab Chip* **2007**, *7*, 1192.
[21] M. Sangermano, S. Marchi, P. Meier, X. Kornmann, *J. Appl. Polym. Sci.* **2013**, *128*, 1521.
[22] A. M. Rivas, S. Suhard, M. Mauzac, A.-F. Mingotaud, C. Séverac, D. Collin, P. Martinoty, C. Vieu, *Microfluid. Nanofluid.* **2010**, *9*, 439.
[23] Carbon3D, Elastomeric polyurethane (EPU 40), http://carbon3d.com/api/files/EPU40_TDS.pdf (accessed: October 2016).
[24] Stratasys, Tangoplus, http://usglobalimages.stratasys.com/Main/Files/Material_Spec_Sheets/MSS_PJ_PJMaterialsDataSheet.pdf?v=635785205440671440 (accessed: October 2016).
[25] Formlabs, Flexible resin, https://formlabs.com/materials/flexible/ (accessed: October 2016).
[26] Spot-A. materials, Spot-A Elastic, http://spotamaterials.com/product/spot-e-1kg/ (accessed: October 2016).

[27] J. Mattia, P. Painter, *Macromolecules* **2007**, *40*, 1546.
[28] J. Park, D. Tahk, C. Ahn, S. G. Im, S. J. Choi, K. Y. Suh, S. Jeon, *J. Mater. Chem. C* **2014**, *2*, 2316.
[29] H. J. Qi, M. C. Boyce, *Mech. Mater.* **2005**, *37*, 817.
[30] A. A. Pawar, G. Saada, I. Cooperstein, L. Larush, J. A. Jackman, S. R. Tabaei, N. J. Cho, S. Magdassi, *Sci. Adv.* **2016**, *2*, e1501381.
[31] E. C. Buruiana, F. Jitaru, A. Matei, M. Dinescu, T. Buruiana, *Eur. Polym. J.* **2012**, *48*, 1976.
[32] K. J. Schafer, J. M. Hales, M. Balu, K. D. Belfield, E. W. Van Stryland, D. J. Hagan, *J. Photochem. Photobiol., A* **2004**, *162*, 497.
[33] L. C. Montemayor, L. R. Meza, J. R. Greer, *Adv. Eng. Mater.* **2014**, *16*, 184.
[34] S. Babaee, J. Shim, J. C. Weaver, E. R. Chen, N. Patel, K. Bertoldi, *Adv. Mater.* **2013**, *25*, 5044.
[35] Y. Jiang, Q. Wang, *Sci. Rep.* **2016**, *6*, 34147.
[36] D. L. Safranski, K. Gall, *Polymer* **2008**, *49*, 4446.
[37] A. M. Ortega, S. E. Kasprzak, C. M. Yakacki, J. Diani, A. R. Greenberg, K. Gall, *J. Appl. Polym. Sci.* **2008**, *110*, 1559.
[38] J. Y. Sun, X. H. Zhao, W. R. K. Illeperuma, O. Chaudhuri, K. H. Oh, D. J. Mooney, J. J. Vlassak, Z. G. Suo, *Nature* **2012**, *489*, 133.
[39] L. L. Harrell, in *Block Polymers: Proceedings of the Symposium on Block Polymers at the Meeting of the American Chemical Society in New York City in September 1969* (Ed: S. L. Aggarwal), Springer, Boston, MA, USA **1970**.
[40] I. W. Jung, J. L. Xiao, V. Malyarchuk, C. F. Lu, M. Li, Z. J. Liu, J. Yoon, Y. G. Huang, J. A. Rogers, *Proc. Natl. Acad. Sci. USA* **2011**, *108*, 1788.
[41] Y. M. Song, Y. Z. Xie, V. Malyarchuk, J. L. Xiao, I. Jung, K. J. Choi, Z. J. Liu, H. Park, C. F. Lu, R. H. Kim, R. Li, K. B. Crozier, Y. G. Huang, J. A. Rogers, *Nature* **2013**, *497*, 95.
[42] R. F. Shepherd, F. Ilievski, W. Choi, S. A. Morin, A. A. Stokes, A. D. Mazzeo, X. Chen, M. Wang, G. M. Whitesides, *Proc. Natl. Acad. Sci. USA* **2011**, *108*, 20400.
[43] R. V. Martinez, J. L. Branch, C. R. Fish, L. H. Jin, R. F. Shepherd, R. M. D. Nunes, Z. G. Suo, G. M. Whitesides, *Adv. Mater.* **2013**, *25*, 205.
[44] M. T. Tolley, R. F. Shepherd, B. Mosadegh, K. C. Galloway, M. Wehner, M. Karpelson, R. J. Wood, G. M. Whitesides, *Soft Rob.* **2014**, *1*, 213.
[45] P. Polygerinos, Z. Wang, J. T. B. Overvelde, K. C. Galloway, R. J. Wood, K. Bertoldi, C. J. Walsh, *IEEE Trans. Rob.* **2015**, *31*, 778.
[46] S. Magdassi, M. Grouchko, O. Berezin, A. Kamyshny, *ACS Nano* **2010**, *4*, 1943.
[47] M. Layani, S. Magdassi, *J. Mater. Chem.* **2011**, *21*, 15378.
[48] Y. Long, J. Wu, H. Wang, X. Zhang, N. Zhao, J. Xu, *J. Mater. Chem.* **2011**, *21*, 4875.
[49] H. W. Kroto, J. R. Heath, S. C. O'Brien, R. F. Curl, R. E. Smalley, *Nature* **1985**, *318*, 162.
[50] I. Cooperstein, M. Layani, S. Magdassi, *J. Mater. Chem. C* **2015**, *3*, 2040.